Nondegenerate phase-conjugate wave via stored atomic coherence based on electromagnetically induced transparency in solids

Zhaohui Zhai, Yiling Dou, Jingjun Xu, and Guoquan Zhang*
The MOE Key Laboratory of Weak Light Nonlinear Photonics, Nankai University, Tianjin 300457, China,
School of Physics, Nankai University, Tianjin 300071, China, and
Applied Physics School, TEDA College, Nankai University, Tianjin 300457, China
(Received 12 November 2010; published 20 April 2011)

A nondegenerate phase-conjugate wave was generated via stored atomic coherence in a Pr^{3+}:Y_2SiO_5 crystal based on the electromagnetically induced transparency effect, and its capability for wave-front reconstruction of phase distortion was demonstrated experimentally. The phase-matching condition during the storage-retrieval process of the phase-conjugate wave was characterized both experimentally and theoretically in detail. Theoretical simulations fit the experimental data very well. Such a scheme of storage and retrieval of the phase-conjugate wave may have potential applications in optical signal processing and information security.

DOI: 10.1103/PhysRevA.83.043825 PACS number(s): 42.50.Gy, 42.65.Hw, 32.80.Qk

I. INTRODUCTION

Optical phase conjugation is one of the various attractive subjects in the field of nonlinear optics [1–4]. It is a very useful and unique method for exploring the nonlinear optical properties of materials and investigating different processes in those media with the action of coherent optical fields. The phase aberration imposed on a beam that passes through an inhomogeneous or disturbing medium can be automatically removed by its backward phase-conjugate wave passing through the same disturbing medium again. This unique feature leads to many prospective applications, such as aberration correction, long-distance optical fiber communications, novel optical data storage and processing systems, etc. Optical phase-conjugate waves can be generated through many nonlinear optical processes (such as four-wave mixing [5], three-wave mixing [6,7], backward stimulated scattering [8–10], etc.) or through photon-pumped backward emission processes in a resonant medium [11–13].

Coherent control of the optical properties of a medium by light fields has been demonstrated in various material systems, such as atoms, molecules, solid-state quantum structures [14], and even the Bose-Einstein condensate [15]. The coherent interaction between light fields and matter based on quantum interference effects provides a powerful way to manipulate the light field, such as its propagation dynamics and the information it carries [16–19]. One of these effects, called electromagnetically induced transparency (EIT), which makes the light propagate through an optically dense medium with almost no absorption and with very low group velocity within a certain frequency window, has attracted much attention [20–22]. Impressive progress on EIT has been made, and various applications based on it have been developed in recent years [23–29]. Particularly, there is growing interest in processing stored light pulses that carry optical information [30] or quantum states [31] or that are even encoded with images based on the EIT effect [32–34].

Recently, Ham *et al.* [35] demonstrated efficient phase-conjugate waves in solids based on the EIT effect, and they found that the conversion efficiency was significantly enhanced due to the EIT effect. Later, Zibrov *et al.* [36] proposed and demonstrated transporting and time reversing of light between different spatial and temporal points via atomic coherence in a coherently prepared atomic vapor. In this paper, we demonstrate the generation of nondegenerate phase-conjugate waves via stored atomic coherence based on the EIT effect, together with its capability for wave-front reconstruction of phase distortion, in a Pr^{3+}:Y_2SiO_5 (YSO) crystal. Furthermore, the phase-matching condition during the storage and retrieval processes of light pulses will be characterized in detail. The phase-conjugate wave of a light pulse retrieved through stored atomic coherence based on the EIT effect has potential applications in optical information processing and optical security.

II. THEORETICAL MODEL

We consider a three-level, Λ-type atomic ensemble consisting of an excited-state level $|a\rangle$ and two ground-state levels $|b\rangle$ and $|c\rangle$, as shown in Fig. 1(a). Based on the EIT effect, a signal pulse E_1 can be stored in the atomic ensemble as the atomic spin coherence grating in the form of a coherent superposition of levels $|b\rangle$ and $|c\rangle$ by adiabatically turning off a coupling field E_2. Here the crossing angle between fields E_1 and E_2 are set to be θ. After a storage time ΔT, we apply a retrieval field E_3 that is of the same frequency as field E_1 but counterpropagates with E_2; a new field E_4 counterpropagating with E_1 will be generated. As we will demonstrate both theoretically and experimentally later on, this new field E_4 is a nondegenerate phase-conjugate wave of field E_1 but with the same frequency as field E_2.

The above coherent interaction between the fields and the atomic ensemble can be described by the motion equation of the density-matrix elements ρ_{mn} of the system [37],

$$\frac{\partial \rho_{mn}}{\partial t} = -\sum_{l=a,b,c}\left[\frac{i}{\hbar}(\mathscr{H}_{ml}\rho_{ln}-\rho_{ml}\mathscr{H}_{ln})+\frac{1}{2}(\gamma_{ml}\rho_{ln}+\rho_{ml}\gamma_{ln})\right], \quad (1)$$

*zhanggq@nankai.edu.cn

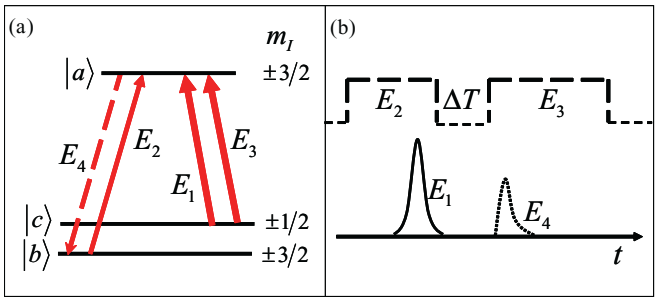

FIG. 1. (Color online) (a) Energy-level diagram of a Λ-type three-level ensemble, consisting of the hyperfine energy levels of the transition $^3H_4 \leftrightarrow {}^1D_2$ of a Pr^{3+} ion in YSO crystal in the experiments. (b) Time sequences of the fields, where the dashed line indicates the on or off state of the coupling field E_2 or the retrieval field E_3, while E_1 and E_4 are the signal pulse and the retrieved phase-conjugate wave, respectively.

where subscripts $m,n = a,b,c$, and the wave equation for field E_4,

$$\left[c^2\nabla^2 - \frac{\partial^2}{\partial t^2}\right] E_4(\mathbf{r},t) = \frac{1}{\epsilon_0}\frac{\partial^2}{\partial t^2} P_{ab}(\mathbf{r},t), \tag{2}$$

where c is the light speed in vacuum and ϵ_0 is the vacuum permittivity. Here $\mathscr{H}$ represents the Hamiltonian of the system

$$\mathscr{H} = \mathscr{H}_0 + \mathscr{H}_1, \tag{3}$$

with

$$\mathscr{H}_0 = \hbar\omega_a|a\rangle\langle a| + \hbar\omega_b|b\rangle\langle b| + \hbar\omega_c|c\rangle\langle c| \tag{4}$$

and

$$\mathscr{H}_1 = -\tfrac{1}{2}(\mu_{ab}E_{ab}|a\rangle\langle b| + \mu_{ac}E_{ac}|a\rangle\langle c|) + \text{H.c.} \tag{5}$$

γ_{mn} and P_{mn} are the relaxation-matrix elements and the polarization of the atomic ensemble associated with the transition $|m\rangle \to |n\rangle$, $\hbar\omega_m$ is the energy eigenvalue of the atomic level $|m\rangle$, $\omega_{mn}(=\omega_m - \omega_n)$ is the resonant frequency of the transition $|m\rangle \to |n\rangle$, and μ_{mn} is the transition dipole moment of the atomic transition. Using the slowly varying amplitude approximation

$$E_s(\mathbf{r},t) = \mathscr{E}_s(\mathbf{r},t)e^{i(\mathbf{k_s}\cdot\mathbf{r}-\nu_s t)} + \text{c.c.}, \tag{6}$$

we define the complex Rabi frequency $\Omega_s = \mu_{mn}\mathscr{E}_s e^{i\mathbf{k_s}\cdot\mathbf{r}}/\hbar$, with $\mathbf{k}_s$ being the wave vector and ν_s being the angular frequency of the field E_s ($s = 1,2,3,4$) coupling the transition $|m\rangle \leftrightarrow |n\rangle$. Then, the interaction part of the Hamiltonian could be rewritten as

$$\mathscr{H}_1 = -\frac{\hbar}{2}(\Omega_{2,4}e^{-i\nu_{2,4}t}|a\rangle\langle b| + \Omega_{1,3}e^{-i\nu_{1,3}t}|a\rangle\langle c|) + \text{H.c.}, \tag{7}$$

where the concrete value of the subscript s (=1, 2, 3, or 4) for Ω_s and ν_s depends on the specific experimental configuration. Equations (1) and (2) are coupled together through the polarization P_{ab} that is related to the off-diagonal density-matrix element ρ_{ab}.

When the coupling field E_2 is adiabatically turned off, the signal pulse E_1 is mapped onto a dark state, a coherent superposition of the ground-state levels $|b\rangle$ and $|c\rangle$ [23]. The amplitude of the stored spin coherence ρ^0_{cb} is proportional to the product of the Rabi frequencies of the two fields,

$$\rho^0_{cb} \propto \Omega_2\Omega_1^* e^{-i\omega_{cb}t}, \tag{8}$$

and it decays exponentially as $\rho_{cb}(t) = \rho^0_{cb}e^{-\gamma_{cb}t}$ with a dephasing rate γ_{cb}.

The stored spin coherence in the atomic ensemble can be transferred to the light field E_4 by applying a retrieval field E_3. By using slowly varying amplitude approximation $\rho_{mn} = \tilde{\rho}_{mn}e^{-i\omega_{mn}t}$ and under the rotating wave approximation, the density-matrix elements $\tilde{\rho}_{ab}$ and $\tilde{\rho}_{cb}$ evolve as

$$d\tilde{\rho}_{ab}/dt = i\Omega_3\tilde{\rho}_{cb} - (\gamma_{ab} + i\delta_4)\tilde{\rho}_{ab}, \tag{9}$$

$$d\tilde{\rho}_{cb}/dt = i\Omega_3^*\tilde{\rho}_{ab} - [\gamma_{cb} - i(\delta_3 - \delta_4)]\,\tilde{\rho}_{cb}. \tag{10}$$

By eliminating $\tilde{\rho}_{cb}$ in the above equations, we can get a second-order differential motion equation for $\tilde{\rho}_{ab}$:

$$\frac{d^2\tilde{\rho}_{ab}}{dt^2} + (\Gamma_{ab} + \Gamma^*_{cb})\frac{d\tilde{\rho}_{ab}}{dt} + (\Gamma_{ab}\Gamma^*_{cb} + |\Omega_3|^2)\tilde{\rho}_{ab} = 0. \tag{11}$$

Here $\Gamma_{ab} = \gamma_{ab} + i\delta_4$ and $\Gamma_{cb} = \gamma_{cb} + i(\delta_3 - \delta_4)$ are complex decay constants, and $\delta_3 = \omega_{ac} - \nu_3$ and $\delta_4 = \omega_{ab} - \nu_4$ are the frequency detunings of E_3 and E_4 with respect to the transitions $|a\rangle \leftrightarrow |c\rangle$ and $|a\rangle \leftrightarrow |b\rangle$, respectively. Here we are interested in field E_4, which is retrieved by applying a retrieval field E_3 after a finite storage time ΔT. In this case, Eq. (11) actually describes a temporal dynamics analogy to the motion of a harmonic oscillator subject to a step-function excitation. When taking the specific parameters for the Pr^{3+} ions in YSO crystal into account [37], we find that the coherence $\tilde{\rho}_{ab}$ behaves as an underdamped harmonic oscillator whose amplitude is gradually decreasing to zero, and it can be expressed as

$$\tilde{\rho}_{ab}(t) = \Omega_3\tilde{\rho}^0_{cb}e^{-\gamma_{cb}\Delta T}\frac{\sinh(ut)}{u}e^{-(\Gamma_{ab}+\Gamma^*_{cb})t/2}, \tag{12}$$

where $4u^2 = (\Gamma_{ab} - \Gamma^*_{cb})^2 - 4\Omega_3\Omega_3^*$.

The polarization of a single atom associated with the transition $|a\rangle \leftrightarrow |b\rangle$ is given by

$$p_{ab}(\mathbf{r},t) = \mu_{ab}\tilde{\rho}_{ab}e^{-i\omega_{ab}t} = \mu_{ab}\rho_{ab}, \tag{13}$$

and the polarization of the atomic ensemble is the sum over all atoms in the ensemble,

$$P_{ab}(\mathbf{r},t) = \sum p_{ab}(\mathbf{r},t) + \text{c.c.} \tag{14}$$

Thus, the retrieved field E_4 is a constructive interference of the emission $|a\rangle \to |b\rangle$ of all atoms in the $\mathbf{k}_4$ direction:

$$E_4(\mathbf{k}_4,t) = \frac{1}{4\pi\epsilon_0(2\pi)^{3/2}}\int \eta(\mathbf{r})\,P_{ab}(\mathbf{r},t)\exp(-i\,\mathbf{k}_4\cdot\mathbf{r})d^3\mathbf{r}. \tag{15}$$

Here $\eta(\mathbf{r})$ is the atomic density at position $\mathbf{r}$, and the integral runs over the whole field-atom interaction volume. As shown by Eqs. (8), (12), (14), and (15), field E_4 is proportional to Ω_1^* but with a frequency ω_{ab} different from that of field E_1, indicating that it is a nondegenerate phase-conjugate wave of field E_1.

Substituting Eqs. (8) and (12)–(14) into Eq. (15), we get

$$E_4(\mathbf{k}_4,t) \propto \int \eta(\mathbf{r})\exp[i(-\mathbf{k}_1 + \mathbf{k}_2 + \mathbf{k}_3 - \mathbf{k}_4)\cdot\mathbf{r}]d^3\mathbf{r}. \tag{16}$$

Here we have omitted the temporal evolution part of $\tilde{\rho}_{ab}$ since the integral only runs over the space. Assuming a uniform atomic density distribution $\eta(\mathbf{r}) = \text{const}$ in the field-atom interaction volume, one gets

$$E_4(\mathbf{k}_4,t) \propto L\,\frac{\sin(|\Delta\mathbf{k}|L/2)}{|\Delta\mathbf{k}|L/2} = L\,\text{sinc}(|\Delta\mathbf{k}|L/2)\,, \qquad (17)$$

where $\Delta\mathbf{k} = -\mathbf{k}_1 + \mathbf{k}_2 + \mathbf{k}_3 - \mathbf{k}_4$ is the phase mismatching and L is the field-atom interaction length. Equation (17) describes the typical rocking curve of the phase-matching condition. The case when $\mathbf{k}_2 + \mathbf{k}_3 = 0$ explicitly shows that field E_4 propagates in the $-\mathbf{k}_1$ direction to satisfy the phase-matching condition, and a backward phase-conjugate wave of field E_1 is generated.

III. EXPERIMENTAL CONFIGURATION

We used a 3-mm, 0.05% praseodymium-doped Y_2SiO_5 crystal with its b axis along the 3-mm side in the experiment, and the crystal was held at 3.4 K in a cryostat. The small inhomogeneous broadening, long coherence time, and large oscillator strength of hyperfine transitions of Pr^{3+} ions in Pr:YSO at cryogenic temperature [37,38] make it an attractive candidate for quantum optics experiments. The hyperfine energy levels of the transition $^3H_4 \leftrightarrow {}^1D_2$ were employed to form the Λ-type configuration in our experiments, as shown in Fig. 1(a), where the frequency difference between two ground states $|b\rangle$ and $|c\rangle$ is 10.2 MHz. The density of Pr^{3+} ions in the crystal was $N = 4.7 \times 10^{18}\,\text{cm}^{-3}$, and the maximum absorption coefficient α was measured to be 13 cm^{-1} for a linearly polarized light at 605.78 nm propagating along the b axis of the crystal.

The experimental setup scheme is shown in Fig. 2. A single frequency laser radiation at 605.78 nm with a bandwidth of 0.5 MHz from a frequency-locked Coherent's 899-29 dye ring laser was split into three beams. One of them was the signal field E_1, while the other two, E_2 and E_3, served as the coupling and the retrieval fields, respectively. Fields E_1 and E_2 propagated along the b axis of the crystal with a small crossing angle θ between them, and field E_3 counterpropagated with E_2. Each beam can be modulated in intensity and shifted in frequency independently by the corresponding accousto-optic modulator. All beams were polarized linearly and in parallel to yield maximal absorption in the crystal and were focused into the crystal through different lenses. The beam spots in the crystal were monitored by a charge-coupled device (CCD) camera to ensure a perfect beam overlap, and the beam spot diameters for E_1, E_2, and E_3 in the crystal were measured to be 260, 400, and 400 μm, respectively. The generated backward phase-conjugate wave E_4 was reflected by a beam splitter ($R : T = 1 : 10$ in intensity) and was recorded by a photomultiplier tube (PMT) for its temporal trace or a CCD for its spatial intensity distribution profile. A reference field E_5 with a small frequency difference δ from the resonant frequency ω_{ab} was introduced, and it propagated collinearly with field E_4 to generate a beat signal. A phase-distortion glass slit was placed, when necessary, in the path of E_1 to study the wave-front reconstruction capability of the phase distortion of the backward phase-conjugate wave E_4, as shown in Fig. 2.

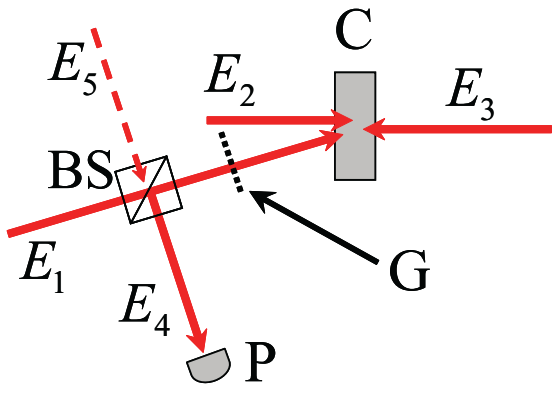

FIG. 2. (Color online) Experimental configuration scheme. Here P is PMT or CCD, G is the phase-distortion glass slit, C is the Pr:YSO crystal, and BS is beam splitter. A reference field E_5 was introduced when necessary to create a beat with the retrieved field E_4.

IV. RESULTS AND DISCUSSIONS

A. Nondegenerate phase-conjugate wave

A spectrally isolated Λ-type three-level ensemble was prepared following the procedures in Refs. [38–40] by combining the optical pumping and spectral hole-burning techniques. This technique permits selectively addressing a well-defined transition in a single ensemble of ions. In the experiments, by adiabatically switching off the coupling beam E_2, a 5-μs, 2-mW Gaussian signal pulse E_1 was stored in the crystal as the atomic coherence of the ensemble, which is a coherent superposition of levels $|b\rangle$ and $|c\rangle$ [30,40,41]. After a storage time ΔT, we applied a retrieval pulse E_3 counterpropagating to field E_2 but with the same frequency as field E_1. The temporal sequence for each pulse is shown in Fig. 1(b). A new field E_4 counterpropagating to field E_1 was generated. As is already shown theoretically in Sec. II and will be verified experimentally in the following, this new field E_4 is a backward nondegenerate phase-conjugate wave of field E_1. We confirmed experimentally that no field would be generated when one launched a retrieval pulse counterpropagating to field E_2 and with the same frequency as field E_2, which is determined by the phase-matching condition during the retrieval process, as we will discuss in detail in Sec. IV B.

A typical temporal trace of the retrieved field E_4 is shown in Fig. 3(a). The retrieved field E_4 increases at first gradually up to a maximum due to the rising polarization of the atomic ensemble driving by field E_3, and then it drops gradually until the stored atomic coherence is completely transferred back to the light field. Figure 3(b) shows the numerically simulated trace based on Eq. (15), where the spectral distribution of field E_3 with a Lorentz line shape and a spectral bandwidth of 0.5 MHz is taken into account. The material parameters used in the simulation are listed in Table I. Note that the relaxation between the ground-state hyperfine levels occurs at a rate of the order of $(100\,\text{s})^{-1}$ and is negligibly small compared to other relaxation processes. One sees that the simulation trace agrees very well with the experimentally measured one.

The frequency of field E_4 was verified to be the same as the resonant frequency ω_{ab} of the transition $|a\rangle \leftrightarrow |b\rangle$ by

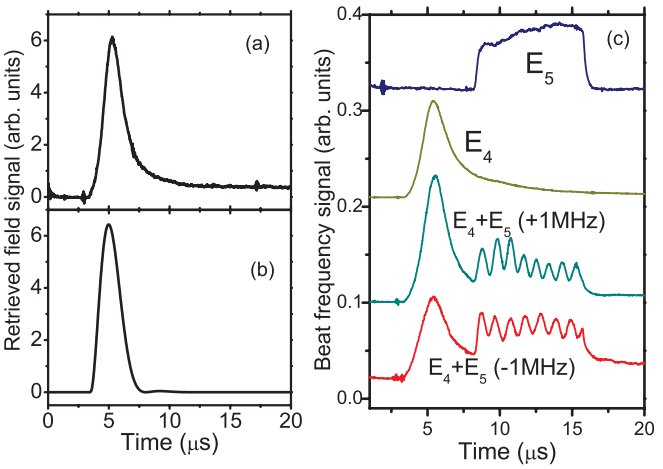

FIG. 3. (Color online) Temporal traces of the retrieved field E_4: (a) experiment, (b) simulation, and (c) the frequency beat between E_4 and the reference field E_5. After a storage time of $\Delta T = 3\,\mu$s, a retrieval field E_3 of 80 W/cm^2 was turned on. In (c), two frequency-beat traces corresponding to frequency differences $\delta = \pm 1.0$ MHz are shown. The traces for E_4 and E_5 are also shown at the top of (c).

employing a frequency-beat technique. A reference field E_5 was introduced and propagated collinearly with field E_4, as shown in Fig. 2. The frequency of the reference field E_5 was shifted by $\delta = \pm 1.0$ MHz with respect to ω_{ab}, and a beat signal with a beating frequency of 1.0 MHz was observed in both cases, as shown in Fig. 3(c), indicating that the frequency of field E_4 is equal to ω_{ab}.

As a phase-conjugate wave of field E_1, field E_4 has the capability of eliminating the phase distortion that field E_1 accumulated during its propagation. To demonstrate this, we placed a phase-distortion glass slit in the path of field E_1. The wave front of E_1 was disturbed after passing through the glass slit, and then it was stored into the crystal and retrieved by applying field E_3 after a storage time ΔT. As a time-reversal wave of field E_1, the retrieved field E_4 passed through the same area of the glass slit again, and the wave front was reconstructed, as shown in Fig. 4(a). For comparison, when the incidence angle of E_3 is slightly detuned (1.7 mrad here) from the phase-matching angle, the retrieved field E_4 would pass through a different area of the glass slit, and the phase distortion would accumulate and become more serious. In this case, the beam spot of E_4 was speckled messily, as shown in Fig. 4(b). Note that the present scheme is based on a storage-retrieval process, and it may have important potential applications in encrypted information storage and communication.

TABLE I. Material parameters for Pr^{3+}:Y_2SiO_5 used in theoretical simulations. Here T_1 and T_2 are the lifetime of the excited state and the decoherence time of the optical transition $|a\rangle \rightarrow |b\rangle$, respectively. γ_{cb} is the coherence relaxation rates for the transition $|c\rangle \rightarrow |b\rangle$. The decoherence time γ_{cb}^{-1}, which is equivalent to the decay time constant τ_{bw}, was measured to be 26 μs in our experiments. Other parameters are from Ref. [37].

T_1 (μs)	T_2 (μs)	γ_{cb}^{-1} (μs)	N (cm^{-3})	$\mu_{ab}(=\mu_{ac})$ (A s m)
164	111	26	4.7×10^{18}	1.20×10^{-32}

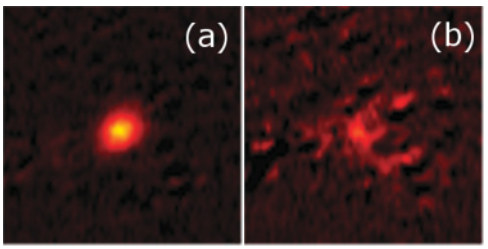

FIG. 4. (Color online) The beam-spot images of the retrieved field E_4 with a phase-distortion glass slit in the path of field E_1. (a) Result with a phase-matched retrieval field E_3 and (b) the case when the retrieval field E_3 is angularly detuned by 1.7 mrad from the phase-matched condition.

The reflectivity η of the phase-conjugate wave E_4, defined as the energy ratio of field E_4 to field E_1, was measured to decay exponentially with the increase of the storage time ΔT, and the decay time constant τ_{bw} of field E_4 was measured to be 26 μs. We also measured the decay time constant τ_{fw} of the stored atomic coherence to be 25.7 μs by reading out the stored atomic coherence with a phase-matched pulse along field E_2 [40]. Note that the two decay time constants coincide with each other very well, indicating that the backward nondegenerate phase-conjugate wave E_4, indeed, originates from the stored atomic coherence. As expected [see Eq. (12)], the reflectivity η of field E_4 increases with the increase in the intensity of E_3 but eventually saturates at ~4% when the stored atomic coherence is transferred completely to the light field, as shown in Fig. 5.

B. Phase-matching condition

Phase-matching conditions are satisfied in various nonlinear optical processes such as four-wave mixing, frequency doubling, and parametric amplification, etc. Due to the phase-matching condition, the constructive interference of

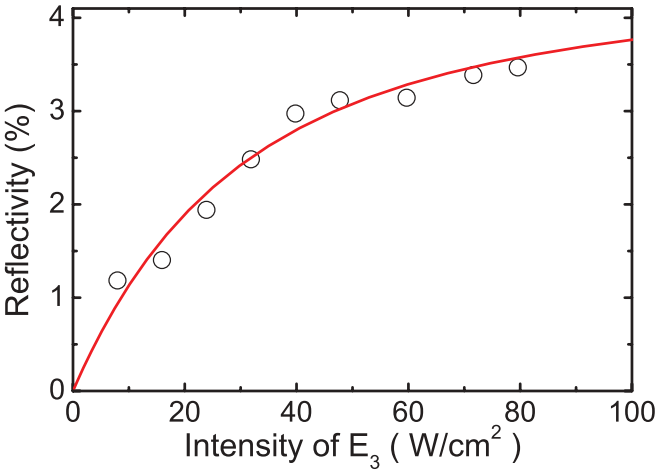

FIG. 5. (Color online) Reflectivity η of field E_4 versus the intensity of field E_3. Open circles are the measured data, and the red solid curve is a theoretical fit based on Eq. (15). Here η was measured at $\Delta T = 0$.

waves generated from different locations yields a maximum efficiency at a specific direction (wave vector) during the nonlinear optical process. The generation efficiency of the new field is sensitively dependent on the phase mismatch $\delta\mathbf{k}$, which can be eliminated by adjusting experimental conditions. In practical applications involving nonlinear optical processes, the phase-matching condition can be satisfied by properly adjusting the incident angles or the frequencies of the involved fields or by tuning the material temperature or simply by using a biaxial crystal to achieve a high efficiency.

The light pulse storage and retrieval based on EIT were reported to satisfy the phase-matching condition, and addressable multichannel buffer memory was proposed and demonstrated [40]. As required by Eq. (17), the phase-matching condition is also satisfied in the retrieval of the nondegenerate phase-conjugate field E_4, and the reflectivity of field E_4 should be highly sensitive to the angular detuning $\Delta\theta$ and the frequency detuning $\delta_3 = \omega_{ac} - \nu_3$ of the retrieval field E_3, where ω_{ac} is the resonant frequency of the transition $|a\rangle \leftrightarrow |c\rangle$ and ν_3 is the frequency of the retrieval field E_3. Such a high sensitivity of the reflectivity to the phase mismatching $\delta\mathbf{k}$ is the base for applications such as multiplexing storage of light pulses and encrypting optical information, whereas it may hinder the technique in certain applications where large tolerance to the phase mismatching is required. In the following subsections, we will give a detailed study of the phase-matching condition during the retrieval process of the nondegenerate phase-conjugate field E_4.

1. Angular detuning

A small angular detuning $\Delta\theta$ of field E_3 from the exact phase-matched incident angle would lead to a finite phase mismatch $\delta\mathbf{k}$, which would make the reflectivity of field E_4 drop rapidly. According to Eq. (17), with a fixed intensity of field E_3, the reflectivity η can be expressed as

$$\eta \propto E_4 E_4^* \propto \left[\frac{\sin(0.5\,|\delta\mathbf{k}|L_{\text{eff}})}{0.5\,|\delta\mathbf{k}|L_{\text{eff}}}\right]^2, \qquad (18)$$

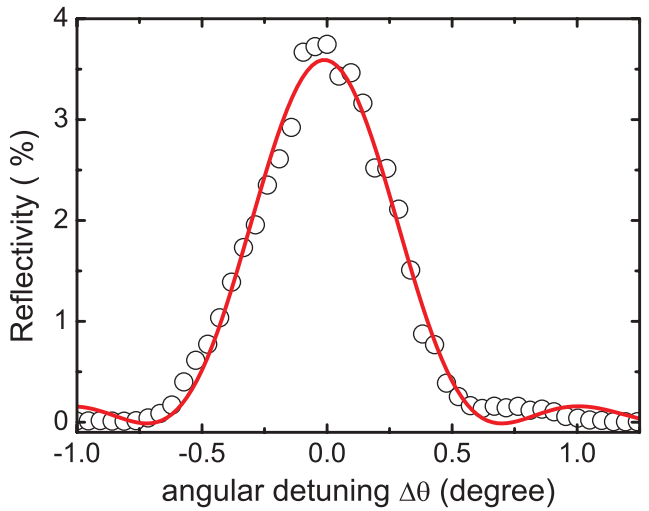

FIG. 6. (Color online) Reflectivity of field E_4 vs the angular detuning $\Delta\theta$ of field E_3. Open circles are the measured data with $\Delta T = 0$, and the red solid curve is the theoretical fit using Eq. (18).

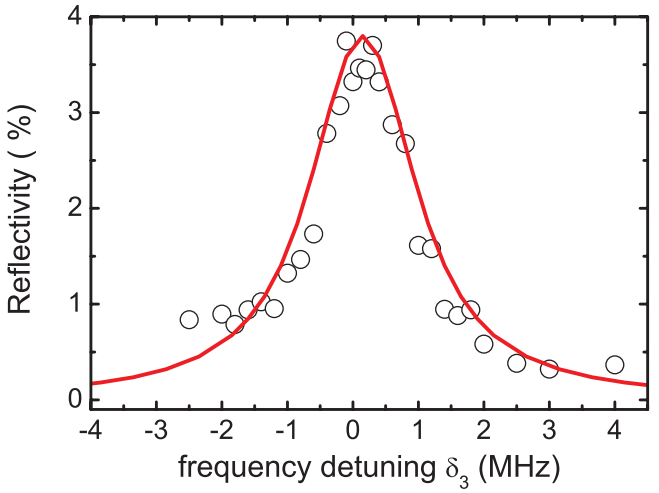

FIG. 7. (Color online) The rocking curve of the reflectivity of field E_4 as a function of the frequency detuning δ_3 of field E_3. Open circles are the experimental data with $\Delta T = 0$, and the red solid curve is a numerical simulation based on Eq. (15) by integrating over the laser spectrum with a Lorentz line shape of a spectral bandwidth of 0.5 MHz.

where the phase mismatch $\delta\mathbf{k} = 4|\mathbf{k}|\sin(\theta/2)\sin(\Delta\theta/2)$ and L_{eff} is the effective interaction length between the fields and the atomic coherence in the crystal. Figure 6 shows the measured angular detuning rocking curve of the reflectivity η (open circles), together with the theoretical fitting curve (red solid curve) using Eq. (18). Note that the frequency of field E_3 was set to be resonant with the transition $|a\rangle \leftrightarrow |c\rangle$. One sees that the experimental results are in good agreement with the theoretical prediction, and the angular resolution of the rocking curve is $\sim 1^\circ$. Furthermore, the effective interaction length L_{eff} is fitted to be 2.85 mm, which is very close to the crystal thickness ($d = 3$ mm).

2. Frequency detuning

Figure 7 shows the rocking curve of the reflectivity of field E_4 as a function of the frequency detuning δ_3 of field E_3. In the experiment, the frequency of field E_3 was detuned from the resonant frequency of the transition $|a\rangle \leftrightarrow |c\rangle$ by an amount of $\delta_3 = \omega_{ac} - \nu_3$, while field E_3 was incident at the phase-matched angle θ. One sees that the reflectivity of field E_4 decreases rapidly with the increase of δ_3. The frequency bandwidth of the frequency detuning rocking curve in Fig. 7 was estimated to be of the order of 1 MHz. Note that the frequency bandwidth of the frequency detuning rocking curve of field E_4 estimated from the phase-matching condition and the angular detuning rocking curve in Fig. 6 should be of the order of terahertz, which is much broader than that shown in Fig. 7. Therefore, mechanisms other than the requirement of the phase-matching condition should be considered. We believe that the narrow frequency bandwidth of the rocking curve in Fig. 7 is mainly the result of the interplay between the bandwidth of the EIT window and the laser spectral linewidth. Both of these two bandwidths are of the order of several hundreds kilohertz, and the overlap between the EIT spectral window and the spectrum of the laser beam itself causes the final frequency detuning rocking curve of the reflectivity to

be on the order of megahertz. The red solid curve in Fig. 7 is a numerical simulation of integrating over the laser spectrum with a Lorentz line shape and a spectral linewidth of 0.5 MHz based on Eq. (15), which describes the frequency detuning rocking curve very well.

V. CONCLUSIONS

In conclusion, a backward nondegenerate phase-conjugate wave was generated in a Pr^{3+}:Y_2SiO_5 crystal based on the stored atomic coherence via electromagnetically induced transparency effect, and its capability for wave-front reconstruction of phase distortion was demonstrated. The reflectivity of the nondegenerate phase-conjugate wave was found to be highly sensitive to the angular detuning of the retrieval field due to the requirement of the phase-matching condition during the storage and retrieval process. However, the frequency detuning rocking curve of the reflectivity of the phase-conjugate wave was determined to be the result of the interplay between the EIT window and the spectral line shape and width of the retrieval field. The experimental measurements are in good agreement with theoretical predictions. These results may have important potential applications in optical information processing and security.

ACKNOWLEDGMENTS

This project is supported by the MOE Cultivation Fund of the Key Scientific and Technical Innovation Project (Grant No. 708022), the NSFC (Grants No. 90922030, No. 10904077, No. 10804054), the 111 project (Grant No. B07013), the 973 program (Grant No. 2007CB307002), the CNKBRSF (Grant No. 2011CB922003), the RFDP (Grant. No. 200800551034), and the Fundamental Research Funds for the Central Universities.

[1] R. Fisher, *Optical Phase Conjugation* (Academic, New York, 1983).
[2] B. Zel'dovich, N. Pilipetsky, and V. Shkunov, *Principles of Phase Conjugation* (Springer-Verlag, Berlin, 1985).
[3] G. He and S. Liu, *Physics of Nonlinear Optics* (World Scientific, Singapore, 2000).
[4] H. Eichler, P. Gunter, and D. Pohl, *Laser Induced Dynamic Gratings* (Springer-Verlag, Berlin, 1986).
[5] D. M. Bloom and G. C. Bjorklund, Appl. Phys. Lett. **31**, 592 (1977).
[6] A. Yariv, Appl. Phys. Lett. **28**, 88 (1976).
[7] A. Yariv, J. Opt. Soc. Am. **66**, 301 (1976).
[8] G. Eckhardt, R. W. Hellwarth, F. J. McClung, S. E. Schwarz, D. Weiner, and E. J. Woodbury, Phys. Rev. Lett. **9**, 455 (1962).
[9] R. Y. Chiao, C. H. Townes, and B. P. Stoicheff, Phys. Rev. Lett. **12**, 592 (1964).
[10] G. S. He and P. N. Prasad, Phys. Rev. A **41**, 2687 (1990).
[11] G. S. He, Y. Cui, M. Yoshida, and P. N. Prasad, Opt. Lett. **22**, 10 (1997).
[12] G. S. He and P. N. Prasad, J. Opt. Soc. Am. B **15**, 1078 (1998).
[13] G. S. He, N. Cheng, P. N. Prasad, D. Liu, and S. H. Liu, J. Opt. Soc. Am. B **15**, 1086 (1998).
[14] T. Amand, V. Blanchet, B. Girard, and X. Marie, *Femtosecond Laser Pulses* (Springer, New York, 2005), pp. 333.
[15] H. Lignier, C. Sias, D. Ciampini, Y. Singh, A. Zenesini, O. Morsch, and E. Arimondo, Phys. Rev. Lett. **99**, 220403 (2007).
[16] N. Ginsberg, S. Garner, and L. Hau, Nature (London) **445**, 623 (2007).
[17] M. S. Bigelow, N. N. Lepeshkin, and R. W. Boyd, Science **301**, 200 (2003).
[18] M. S. Bigelow, N. N. Lepeshkin, and R. W. Boyd, Phys. Rev. Lett. **90**, 113903 (2003).
[19] I. Bloch, Nature (London) **453**, 1016 (2008).
[20] K.-J. Boller, A. Imamoglu, and S. E. Harris, Phys. Rev. Lett. **66**, 2593 (1991).
[21] B. Ham, P. Hemmer, and M. Shahriar, Opt. Commun. **144**, 227 (1997).
[22] S. E. Harris, Phys. Today **50**, 36 (1997).
[23] M. Fleischhauer and M. D. Lukin, Phys. Rev. Lett. **84**, 5094 (2000).
[24] M. Fleischhauer, A. Imamoglu, and J. P. Marangos, Rev. Mod. Phys. **77**, 633 (2005).
[25] P. Arve, P. Jänes, and L. Thylén, Phys. Rev. A **69**, 063809 (2004).
[26] G. Nikoghosyan, Eur. Phys. J. D **36**, 119 (2005).
[27] R. M. Camacho, C. J. Broadbent, I. Ali-Khan, and J. C. Howell, Phys. Rev. Lett. **98**, 043902 (2007).
[28] M. D. Lukin and A. Imamoglu, Nature (London) **413**, 273 (2001).
[29] L. V. Hau, S. E. Harris, Z. Dutton, and C. H. Behroozi, Nature (London) **397**, 594 (1999).
[30] C. Liu, Z. Dutton, C. H. Behroozi, and L. V. Hau, Nature (London) **409**, 490 (2001).
[31] T. Chaneliere, D. Matsukevich, S. Jenkins, S. Lan, T. Kennedy, and A. Kuzmich, Nature (London) **438**, 833 (2005).
[32] M. Shuker, O. Firstenberg, R. Pugatch, A. Ron, and N. Davidson, Phys. Rev. Lett. **100**, 223601 (2008).
[33] P. K. Vudyasetu, R. M. Camacho, and J. C. Howell, Phys. Rev. Lett. **100**, 123903 (2008).
[34] G. Heinze, A. Rudolf, F. Beil, and T. Halfmann, Phys. Rev. A **81**, 011401 (2010).
[35] B. S. Ham, P. R. Hemmer, and M. S. Shahriar, Phys. Rev. A **59**, R2583 (1999).
[36] A. S. Zibrov, A. B. Matsko, O. Kocharovskaya, Y. V. Rostovtsev, G. R. Welch, and M. O. Scully, Phys. Rev. Lett. **88**, 103601 (2002).
[37] E. Kuznetsova, O. Kocharovskaya, P. Hemmer, and M. O. Scully, Phys. Rev. A **66**, 063802 (2002).
[38] M. Nilsson, L. Rippe, S. Kröll, R. Klieber, and D. Suter, Phys. Rev. B **70**, 214116 (2004).
[39] F. Beil, J. Klein, G. Nikoghosyan, and T. Halfmann, J. Phys. B **41**, 074001 (2008).
[40] Y. Tu, G. Zhang, Z. Zhai, and J. Xu, Phys. Rev. A **80**, 033816 (2009).
[41] D. F. Phillips, A. Fleischhauer, A. Mair, R. L. Walsworth, and M. D. Lukin, Phys. Rev. Lett. **86**, 783 (2001).